

sumption that the recoilless fractions of ThO₂ and Th metal were approximately equal. A summary of the results can be found in Table III.

The natural linewidth determined for the first excited state, after corrections were made for broadening due to the geometry of the experimental configuration and for self-absorption in the source, agreed with previous Mössbauer measurements but was slightly broader than would be expected from

previous electronic half-life measurements. Experiments made at about 40 and 78 °K were consistent with the Mössbauer results at 30 °K.

No significant isomer shift was measured; no hyperfine structure was observed. RACE observations carried out on a ThN absorber at 78 °K indicated a linewidth at least as broad as with a ThO₂ absorber.

*Work supported in part by the National Science Foundation.

¹J. A. Stone, Intern. At. Energy Agency, Tech. Rept. Ser. 50, 179 (1966).

²J. A. Stone and W. L. Pillinger, Phys. Rev. 165, 1319 (1968).

³B. D. Dunlap, M. B. Brodsky, G. M. Kalvius, G. K. Shenoy, and D. J. Lam, J. Appl. Phys. 40, 1495 (1968).

⁴G. M. Kalvius, S. L. Ruby, B. D. Dunlap, G. K. Shenoy, D. Cohen, and M. B. Brodsky, Phys. Letters 29B, 489 (1969).

⁵S. L. Ruby, G. M. Kalvius, B. D. Dunlap, G. K. Shenoy, D. Cohen, M. B. Brodsky, and D. J. Lam, Phys. Rev. 184, 374 (1969).

⁶J. R. Oleson, Y. K. Lee, J. C. Walker, and J. W. Wiggins, Phys. Letters 25B, 258 (1967).

⁷N. Hershkowitz, C. G. Jacobs, Jr., and K. A. Murphy, Phys. Letters 27B, 563 (1968).

⁸R. E. Bell, S. Bjornholm, and J. C. Severiens, Kgl. Danske Videnskab. Selskab, Mat.-Fys. Medd. 32, No. 12 (1960).

⁹J. H. Hamilton, A. V. Ramayya, B. von Nooijen, R. G. Allbridge, E. F. Zganjar, S. C. Pancholi, J. M. Hollander, V. S. Shirley, and C. M. Lederer, Nucl. Data 1, 521 (1966).

¹⁰C. J. Jacobs and N. Hershkowitz, Phys. Rev. B 1, 839 (1970).

¹¹S. Wender, L. W. Oberley, and N. Hershkowitz, Nucl. Instr. Methods 89, 61 (1970).

¹²E. K. Storms, *The Refractory Carbides* (Academic, New York, 1967).

¹³A. J. F. Boyle and H. E. Hall, Rept. Progr. Phys. 25, 441 (1962).

¹⁴A. H. Muir, Jr., K. J. Ando, and H. M. Coogan, *Mössbauer-Effect Data Index 1958-1965* (Interscience, New York, 1966).

¹⁵M. W. Mekshes and N. Hershkowitz, Phys. Rev. C 2, 289 (1970).

¹⁶N. Hershkowitz, Nucl. Instr. Methods 53, 172 (1967).

¹⁷F. Aramu and V. Maxia, Nucl. Instr. Methods 80, 35 (1970).

Nuclear-Resonance Studies of Critical Fluctuations in FeF₂ above T_N^*

Albert M. Gottlieb[†] and Peter Heller

Physics Department, Brandeis University, Waltham, Massachusetts 02154

(Received 22 January 1971)

A detailed experimental study is made of the behavior of the F¹⁹ nuclear-resonance linewidth in the paramagnetic state of the uniaxial anisotropic antiferromagnet FeF₂. It is concluded that the observed linewidths are due to nuclear-electronic hyperfine interaction modulated by electron-spin motion. The portion $\delta\nu_{||}$ of the linewidth due to the longitudinal component of the local field fluctuation is determined. The critical behavior of $\delta\nu_{||}$ is found to be described by a power law $\delta\nu_{||} \propto (T - T_N)^{0.67 \pm 0.02}$ for $0.04 < T - T_N < 1.5$ °K. This is in good agreement with predictions based on the extension by Riedel and Wegner of the dynamical-scaling theory to anisotropic systems.

I. INTRODUCTION

We have made detailed measurements of the F¹⁹ nuclear magnetic resonance (NMR) linewidth in the paramagnetic state of the anisotropic antiferromagnet FeF₂. A pronounced anomaly is observed near the critical temperature $T_N = 78.366$ °K. Our data provide information on the statics and dynamics of

the critical fluctuation behavior.

Over the past few years, there has been considerable interest in the broad range of phenomena taking place near critical points.¹⁻³ Let us now briefly summarize these facts in a qualitative way, with reference to an antiferromagnet such as FeF₂. The order parameter, i.e., the sublattice magnetization,⁴ approaches zero as the critical point $T_c = T_N$

is approached from below, and remains zero for $T > T_c$. While long-range antiferromagnetic order is absent above T_c , short-range order is present. We may discuss this physically by imagining that a snapshot picture of the spin system was taken. We would observe clusters of alternately oriented spins. The average cluster size, i. e., the correlation length $\xi = \kappa^{-1}$, increases as T_c is approached from above. Also, the mean-squared amplitude of the staggered (alternating) Fourier component of the magnetic-moment distribution increases; it follows that the staggered susceptibility increases as $T \rightarrow T_c$.

The properties just discussed are static properties, i. e., they are fully described by the wavelength-dependent static susceptibilities⁵ $\chi(\vec{K})$. Of equal interest are the dynamical aspects of the critical fluctuations. Thus, in our physical picture we should consider the average lifetime of the "clusters"; we may expect this time to increase as T_c is approached.⁶ The analogous phenomena in fluids have been investigated by means of light-scattering experiments.⁷ In magnetic systems, the simplest theory of this critical slowing-down, the so-called "conventional theory," predicts that for the staggered mode ($\vec{K} = \vec{K}_0$) the relaxation rate $\Gamma(\vec{K}_0)$ should be inversely proportional to the staggered susceptibility⁸ $\chi(\vec{K}_0)$. The slowing of the staggered-mode fluctuation was first demonstrated qualitatively by Nathans, Menzinger, and Pickart⁹ for the isotropic antiferromagnet RbMnF_3 , using inelastic neutron scattering. Subsequent accurate work by Lau *et al.*¹⁰ showed that the conventional theory is quantitatively incorrect. A much better description of the observed slowing-down is provided by the theory of dynamical scaling.^{11,12} In this theory, proposed originally for the case of liquid helium by Ferrel and coworkers,¹¹ and extended and applied to magnetic systems by Halperin and Hohenberg,¹² it is assumed that the ratio $\Gamma(\vec{q} + \vec{K}_0, T)/\Gamma(\vec{K}_0, T)$ depends only on the ratio $q/\kappa(T)$ in the critical region. This theory^{12,13} is in remarkably good accord with the data¹⁰ on RbMnF_3 , an isotropic antiferromagnet.

Recently, the dynamical-scaling theory has been extended to the case of anisotropic systems by Riedel and Wegner.¹⁴ For FeF_2 , they predict that for the range of temperatures closest to T_N , the conventional behavior $\Gamma_{||}(\vec{K}_0) \propto \chi_{||}(\vec{K}_0)^{-1}$ should be seen for the longitudinal fluctuation. Their theory can also be used to predict the temperature dependence of the NMR linewidth in FeF_2 ; we shall see in Sec. V that this prediction is in remarkably good accord with our experiments. A preliminary account of this was given earlier.¹⁵

Inelastic neutron scattering provides the primary experimental tool for investigating the wavelength-dependent relaxation behavior. Such a study on

FeF_2 has recently been reported by Schulhof, Hutchings, and Guggenheim.¹⁶ This experiment followed an earlier study¹⁷ of MnF_2 , a weakly anisotropic antiferromagnet. The limiting factor in such an experiment is the instrumental resolution. This becomes more and more important when, as T_c is approached, the energy spread of the scattered neutron beam becomes smaller and smaller. This is particularly true in FeF_2 where the near-critical fluctuations are unusually slow.¹⁶ There is thus a region of the $(\kappa_{||}, q)$ plane surrounding the origin which is inaccessible to neutrons.

Measuring the width of an NMR absorption line provides both an alternate and a complementary approach.^{18,19} We will see how it is possible to determine the portion of the NMR linewidth $\delta\nu_{||}(T)$ which is due to the longitudinal spin fluctuations. Physically, the critical anomaly in $\delta\nu_{||}(T)$ is due to the increased fluctuation amplitudes, as expressed by the reduced longitudinal static susceptibilities $\chi_{||}(\vec{K})$, together with the slowing-down, as expressed by the decreased longitudinal relaxation rates $\Gamma_{||}(\vec{K}, T)$. This may be written^{3,19,20} as

$$\delta\nu_{||}(T) = C \int d^3K \frac{|A(\vec{K})|^2 \chi_{||}(\vec{K})}{\Gamma_{||}(\vec{K})}, \quad (1)$$

where $A(\vec{K})$ and the constant C may be calculated from the known nuclear-electronic hyperfine interactions and other known parameters. As long as $\delta\nu_{||}$ is small enough to provide a measurable NMR line, the information on the right side of (1) may be obtained. In practice, lines of width up to 10^7 Hz can be studied using present signal-processing techniques.

It is important to note that the nuclei sense the fluctuations at a single spacial location. This is expressed in (1) where we note that only an *integral* over wave vectors is obtained. We shall see, however, that in cases where supplementary information on the wavelength dependence of the integrand is available, either from a theory (such as dynamical scaling) or from scattering experiments, that data for $\delta\nu_{||}$ are very valuable. Thus we will see that the present NMR data support the conclusions of the Riedel-Wegner¹⁴ theory down to within 0.04°K of the critical point. At this temperature $\delta\nu_{||}$ is dominated by modes whose spectral widths are well inside the resolution available in the scattering experiments.

In principle, given properly resolution-corrected and absolutely calibrated neutron scattering data at all wave vectors \vec{K} , it should be possible to *calculate* $\delta\nu_{||}$ from (1). We have, in fact, made such a quantitative comparison of the MnF_2 scattering data of Ref. 13 with the NMR measurements^{18,19} in that material. This comparison has been described²¹ in detail by one of us (A. M. G.) and will be published

separately. We feel that such a quantitative comparison between the NMR and neutron scattering techniques may also serve as a useful check.

II. EXPERIMENTAL TECHNIQUES

All measurements²² were made on a high-quality oriented single crystal of FeF_2 grown by Dr. Stanle Reed and kindly supplied to us by Professor J. W. Stout. This is the same sample used by Kulpa in his NMR measurement⁴ of the temperature dependence of the sublattice magnetization below T_N .

Temperatures, controlled to within ~ 0.001 °K by feedback techniques, were measured with a calibrated platinum resistance thermometer corrected for magnetoresistance effects. The slight effect of the applied field in shifting the critical temperature was also considered with the aid of the data of Shapira.²³ All our linewidth data are given as a function of $T - T_N(\vec{H})$. The zero-field critical temperature was obtained experimentally (using exactly the same thermometer and low-temperature geometry as in the linewidth measurements) by observing the F^{19} resonance behavior just below T_N . This gave

$$T_N = (78.366 \pm 0.003) \text{ °K.} \quad (2)$$

Standard field-modulation and derivative detection techniques were used, with a digital signal averager (used for up to 20 h) following the phase-sensitive detector. Magnetic field sweep was used throughout, with field-swept linewidths converted into frequency units through a knowledge²⁴ of the effective temperature-dependent magnetogyric ratio for the F^{19} resonance. In analyzing the magnetic field sweeps, we fitted the signal-versus-field data to the derivative of a Lorentzian shape function using a least-squares procedure. A term corresponding

to a linear base-line drift (whose origin was the vibrations induced by the eddy currents set up by the field modulation) was also included. This was important very close to T_N .

Corrections were made for the effect of finite-field modulation amplitude.²⁵⁻²⁷ The orientation of the applied field \vec{H}_0 relative to the crystal axes was also considered very carefully to make sure that the observed linewidths correspond accurately to the cases $\vec{H}_0 \parallel c$ or $\vec{H}_0 \parallel a$.

III. RESULTS

In Fig. 1 we show our results for the F^{19} linewidth above T_N . These data were taken in an applied field $\vec{H}_0 \approx 3.8$ kG oriented either along the c axis (squares) or a axis (circles), and will be referred to as $\delta\nu_c$ or $\delta\nu_a$, respectively. The indicated error limits were assigned on the following basis: To the statistical error in fitting the lines to a Lorentzian shape we have added an allowance of 1 or 2% of the linewidth for the uncertainty in our field-sweep calibration, together with an allowance of 20% of the field-modulation correction, and an additional allowance for possible slight sample misalignment. The statistical error, which was usually by far the largest contribution, corresponds to two standard deviations (95% confidence level).

In all cases the measured linewidths refer to the spacing in frequency between absorption derivative extrema. This corresponds to the transverse relaxation time T_2 through the relation

$$\delta\nu = (\pi\sqrt{3} T_2)^{-1}. \quad (3)$$

These results are discussed in Secs. IV and V.

Some additional data, taken in higher applied fields, $\vec{H}_0 \approx 15$ kG, are presented in Fig. 2. The squares and circles again correspond to measure-

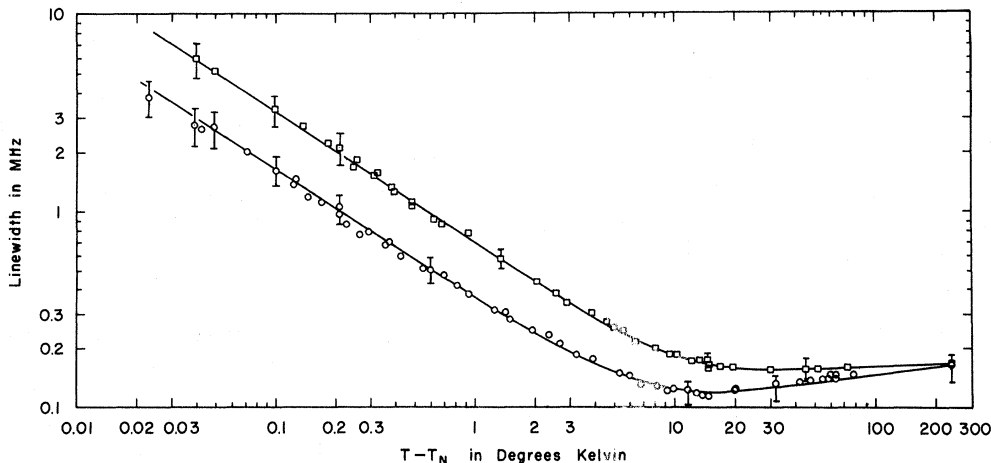


FIG. 1. Measured F^{19} linewidths in FeF_2 for $78.388 < T < 300$ °K. These data were taken in an applied field $H_0 \approx 3.8$ kG oriented either along the c axis (upper squares) or a axis (lower circles).

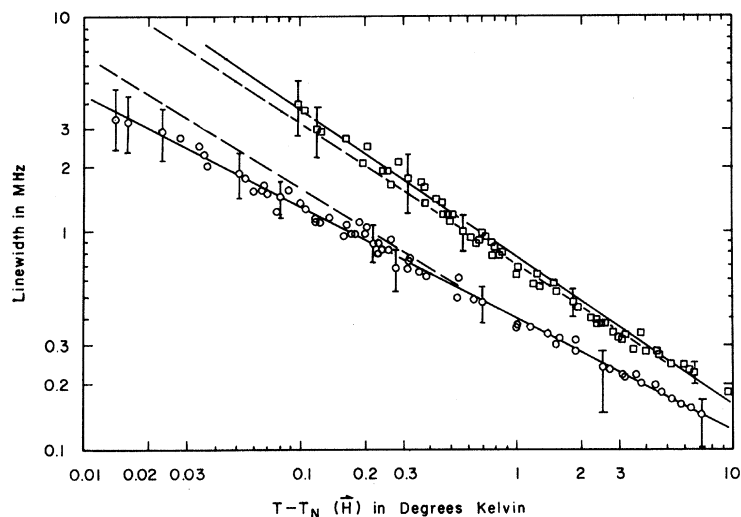


FIG. 2. F^{19} linewidths measured in a relatively high applied field $H_0 \approx 15$ kG directed either along the c axis (upper squares) or a axis (lower circles). The dashed lines correspond to the smoothed low-field data of Fig. 1.

ments made with \vec{H}_0 along c or along a , respectively. The dashed lines correspond to the smoothed data taken at 3.8 kG. The basis for the assignment of the error limits is the same as for the 3.8-kG data, although the 15-kG data are less accurate since a number of technical improvements were made in the apparatus for the 3.8-kG experiment. The importance of 15-kG data is to see whether the 3.8-kG data really constitute a measurement of the NMR linewidth with zero field acting on the Fe^{2+} spin system. In Fig. 2 we do see a slight field effect, tending to lower $\delta\nu_c$ and raise $\delta\nu_a$ as H_0 is decreased from 15 to 3.8 kG, especially near T_N . However, if the effect were linear in H_0 (or, more likely, quadratic at low fields), it is clear that a further decrease of H_0 from 3.8 kG to ≈ 0 should produce an insignificant change. Thus we conclude that the effect on the Fe^{2+} spin system of the 3.8-kG field used in obtaining the data of Fig. 1 is quite small.

IV. RELATION OF LINEWIDTH TO FLUCTUATING LOCAL FIELD

A. Linewidth Broadening Mechanisms

The physical mechanisms that have been discussed in connection with the critical anomaly in the NMR linewidth include (a) the effect of the hyperfine interaction modulated by electron-spin motion,^{20, 28, 29} (b) the indirect nuclear-nuclear coupling via the hyperfine interaction,²⁰ and (c) spacial inhomogeneity of the time-averaged local field.¹⁹ We believe the first of these mechanisms, which is expressed by the Kubo-Tomita formula,^{28, 29} to be by far the dominant cause of the anomaly we observe in FeF_2 . In Sec. IV B we will review the formulas describing mechanism (a) in detail, and show how the part of the observed linewidth $\delta\nu_c$ due to the c component

of the local field fluctuation may be deduced from the measured values of $\delta\nu_c$ and $\delta\nu_a$. This is of interest since it is the c component of the spin fluctuation that undergoes an anomaly in the critical region.

We first sketch the nature of these three mechanisms, and present the evidence indicative of the dominance of mechanism (a). This mechanism may be described physically by noting that fluctuations in the local hyperfine field produce nuclear relaxation by disturbing the otherwise uniform nuclear Larmor precession. An analysis of this effect shows that if, as is surely the case in FeF_2 just above T_N , the local field fluctuation is essentially in the c direction, then the linewidth is doubled upon rotating the Larmor precession axis from c to a . In other words we have

$$\delta\nu_c/\delta\nu_a = 2.00. \quad (4)$$

This prediction is in good accord with our low-applied-field data: Note in Fig. 1 that the spacing between the drawn lines corresponds exactly to a factor of 2 for $|T - T_N| < 1.5^\circ K$. We should stress that this linewidth anisotropy has nothing to do with the effect of the field on the Fe^{2+} spin system. It is precisely the anisotropy that would occur if somehow the field could be applied to the F^{19} nuclei alone.

Mechanism (b) may be described physically by noting that the static wavelength-dependent susceptibilities for the electron-spin system become large in the critical region. It follows that a field applied to a single electron spin will produce an increasingly stronger and longer-ranged disturbance as $T \rightarrow T_N$. In effect, a given nucleus applies such a field via the hyperfine interaction. The resulting disturbance in the electron-spin system affects other nuclei. Thus there is an effective nuclear-

nuclear coupling³⁰ which is strongly enhanced²⁰ as the critical temperature is approached.

For the case of MnF_2 , Moriya²⁰ considered this critical enhancement in detail. He estimated how both the effective F^{19} - F^{19} coupling and the effective F^{19} - Mn^{55} coupling contributed to the second moment of the F^{19} resonance. For $\vec{H}_0 \parallel c$, his results may be written³¹

$$[\langle(\delta\nu)^2\rangle]_{\text{F}^{19}\text{-F}^{19}}^{1/2} \cong 1.5 \epsilon^{-\nu/2} \text{ kHz} \quad (5a)$$

and

$$[\langle(\delta\nu)^2\rangle]_{\text{F}^{19}\text{-Mn}^{55}}^{1/2} \cong 20 \epsilon^{-\nu/2} \text{ kHz} . \quad (5b)$$

Here $\epsilon = (T - T_N)/T_N$ and $\nu = \frac{1}{2}$ is the critical index for the inverse correlation length in this mean-field calculation. Since only the *static* wavelength-dependent susceptibilities entered Moriya's calculations, it is not difficult to modify his results so as to be in harmony with the experimentally observed critical susceptibility behavior. To do this it suffices to observe that while the temperature dependence of the inverse correlation length is poorly described by mean-field theory, the Ornstein-Zernike form for the wavelength dependence is still a quite good approximation.³² Thus, for the value of the inverse correlation length that entered the calculations leading to (5), we should put in the *experimental* value

$$\kappa_{\parallel}(T) = \kappa_* \epsilon^{\nu}.$$

Here $\nu \approx \frac{2}{3}$, while the coefficient κ_* is still roughly that obtained in mean-field theory.

To describe FeF_2 , we note that the Fe^{2+} - F^{19} interaction is only slightly larger than the Mn^{2+} - F^{19} interaction in MnF_2 , but that the Fe^{2+} - Fe^{57} interaction is well over an order of magnitude smaller than the Mn^{2+} - Mn^{55} interaction in MnF_2 . In addition we note that Fe^{57} —the only iron isotope with a nonzero nuclear moment—is only 2.2% abundant. From this it is clear that the effective F^{19} - Fe^{57} coupling will not be significant. An estimate of mechanism (b) in FeF_2 can thus be obtained simply by modifying (5a) to read

$$\begin{aligned} [\langle(\delta\nu)^2\rangle]_{\text{mechanism (b)}}^{1/2} &\lesssim 3 \epsilon^{-1/3} \text{ kHz} \\ &\approx 13 (T - T_N)^{-1/3} \text{ kHz}. \end{aligned} \quad (6)$$

This is for $\vec{H}_0 \parallel c$. For $\vec{H}_0 \parallel a$ we may expect the linewidth to be smaller by about a factor of 2.³¹ On comparison with the experimental linewidths of Fig. 1 we see that our estimate of mechanism (b) is smaller by a factor of at least 50 for $T_N < T < T_N + 10^\circ\text{K}$. Thus even allowing for substantial error in the relatively crude calculations leading to (6), it is clear that mechanism (b) is not important.

Now consider mechanism (c). This may be expected to be important *below* T_N . Indeed, if the local value of the critical temperature varied from one part of the sample to another, the very large

time-averaged local field would also vary. The magnitude of this effect should be proportional to the slope of the sublattice-magnetization-versus-temperature curve. Observations on MnF_2 just below T_N were consistent with this picture.¹⁹ Above T_N , on the other hand, the contribution of the hyperfine interaction to the time-averaged local field amounts to no more than about 7% of the applied field. For $H_0 = 3.8 \text{ kG}$, this is about 270 G. It is conceivable that this amount might be a function of position, at least near impurities. The resulting effect on the linewidth would depend on the applied field, vanishing as $H_0 \rightarrow 0$. But we have seen in Sec. III that the effect of the 3.8-kG field used in taking the data of Fig. 1 is insignificant. Accordingly we will interpret our 3.8-kG data on the basis of mechanism (a) which we now discuss in detail.

B. Linewidth Due to Fluctuating Hyperfine Interaction

1. Condition for Lorentzian Line Shape: Linewidth Formulas

Let the interaction of a nucleus \vec{I} with the electron-spin system be of the form

$$\mathcal{H}_{\text{hf}} = [\langle\vec{V}\rangle + \delta\vec{V}] \cdot \vec{I} \quad (7)$$

Thus, for example, for coupling to a single electron spin \vec{S} through an isotropic interaction $A_{\text{hf}} \vec{I} \cdot \vec{S}$, we would have $\langle\vec{V}\rangle = A_{\text{hf}} \vec{S}$, $\delta\vec{V} = A_{\text{hf}} \delta\vec{S}$. (Here Dirac brackets denote a thermal average, and $\delta A = A - \langle A \rangle$ for any dynamical variable A .) More generally, we can think of $\langle\vec{V}\rangle / (-\gamma_n \hbar)$ as the average local field at a nucleus with $\delta\vec{V} / (-\gamma_n \hbar)$ as the fluctuating part of the local field. Here $\gamma_n = \omega_0 / |H_{\text{nucel}}|$ is the nuclear magnetogyric ratio.

Using the Kubo-Tomita²⁸ formalism, Moriya²⁹ obtained a general expression for the NMR line shape in terms of the correlation functions for the components of $\delta\vec{V}$. In particular it was shown that a Lorentzian shape is obtained provided that the nuclear relaxation still remains slow in comparison with both the local field fluctuations and the Larmor precession. If these conditions are satisfied, the transverse nuclear relaxation time T_2 and the NMR linewidth $\delta\nu$ between derivative extrema are given by

$$\begin{aligned} \pi\sqrt{3} \delta\nu = \frac{1}{T_2} = \frac{1}{2\hbar^2} \int_{-\infty}^{\infty} dt [\langle\{\delta\vec{V}_z(t) \delta\vec{V}_z(0)\}\rangle \\ + \frac{1}{2} e^{i\omega_0 t} \langle\{\delta V_+(t) \delta V_-(0)\}\rangle]. \end{aligned} \quad (8)$$

Here ω_0 is the Larmor (angular) frequency, z is along the direction of the average local field, and $\delta V_{\pm} = \delta V_x \pm i\delta V_y$. The curly brackets stand for a symmetrized product, i. e., $\{AB\} = \frac{1}{2}(AB + BA)$.

Using (8) we would like to discuss how the observed linewidth $\delta\nu$ should depend on the direction of the time-averaged local field. In practice, of

course, it is impossible to apply a field to the nuclei without also putting a field on the electron-spin system. Here we will simply assume that the field used in the experiments had practically no effect on the electron-spin system. If this is correct, then the electron-spin correlation functions, and hence the local field correlation functions, are unaffected by the field and may be set equal to their zero-field forms. More precisely we assume that the effect of the field is expressed only by the very slight shift in the critical temperature. This is the situation expected for the static susceptibilities $\chi(\vec{K})$, at least, in mean-field theories of antiferromagnets.^{33,34} As discussed in Sec. III, this is apparently the case in FeF_2 for $H_0 \cong 3.8$ kG, at least at the level of accuracy of our linewidth data. It may not be the case for $H_0 \cong 15$ kG, however.

It is convenient to express the linewidth in terms of the quantities

$$J_{\alpha\beta}(\omega) = (1/\pi) \int_{-\infty}^{\infty} \langle \{\delta V_{\alpha}(t) \delta V_{\beta}(0)\} \rangle \cos \omega t dt, \quad (9)$$

where α, β denote Cartesian components. Also write

$$J(\omega) = (1/\pi) \int_{-\infty}^{\infty} \langle \{\delta \vec{V}(t) \cdot \delta \vec{V}(0)\} \rangle \cos \omega t dt. \quad (10)$$

Physically $J_{\alpha\alpha}(\omega)/(\gamma_n^2 \hbar^2)$ is the spectral density of the α component of the fluctuating local field. Then (8) becomes essentially³⁵

$$\pi \sqrt{3} \delta\nu = \frac{1}{T_2} = \frac{\pi}{2\hbar^2} [J_{zz}(0) + \frac{1}{2} J_{xx}(\omega_0) + \frac{1}{2} J_{yy}(\omega_0)], \quad (11a)$$

or equivalently³⁶

$$\pi \sqrt{3} \delta\nu = \frac{1}{T_2} = \frac{\pi}{2\hbar^2} [J_{zz}(0) - \frac{1}{2} J_{zz}(\omega_0) + \frac{1}{2} J(\omega_0)]. \quad (11b)$$

Thus we have related the observed linewidth to the power spectrum of the local field fluctuations. With this notation the conditions for obtaining a Lorentzian line shape described by these formulas may be stated compactly as

$$|J_{\alpha\beta}(0) - J_{\alpha\beta}(T_2^{-1})| \ll J_{\alpha\beta}(0) \quad (12)$$

and

$$\omega_0 T_2 = (2/\sqrt{3}) \nu / \delta\nu \gg 1. \quad (13)$$

2. Behavior for Low Larmor Frequencies: Case of Tetragonal Symmetry: Derivation of Longitudinal Fluctuation Contribution $\delta\nu_{\parallel}$

Suppose that the Larmor frequency is high enough to satisfy (13) but low enough so that we can write

$$|J_{\alpha\beta}(0) - J_{\alpha\beta}(\omega_0)| \ll J_{\alpha\beta}(0). \quad (14)$$

Then (11a) can be written

$$\delta\nu = (2\hbar^2\sqrt{3})^{-1} [J_{zz}(0) + \frac{1}{2} J_{xx}(0) + \frac{1}{2} J_{yy}(0)]. \quad (15)$$

In this case³⁶ the ratio of linewidths for any two orientations of the Larmor precession axis cannot exceed 2. If only one Cartesian component of the local field fluctuation is large, the effect of changing the Larmor precession axis from that direction to a transverse direction will be to decrease $\delta\nu$ by a factor of 2. This is evidently the situation near and above T_N in FeF_2 , as noted in (4).

We now consider the case of tetragonal crystals such as MnF_2 and FeF_2 . Taking a coordinate system along the crystalline axes a, a' , and c , we note that the symmetry at each F^{19} site is such that

$$J_{aa} = J_{a'a'}.$$

It follows that the linewidths with the Larmor precession axis, respectively along c and a , can be written

$$\delta\nu_c = (2\hbar^2\sqrt{3})^{-1} [J_{cc}(0) + J_{aa}(0)], \quad (16)$$

$$\delta\nu_a = (2\hbar^2\sqrt{3})^{-1} [\frac{3}{2} J_{aa}(0) + \frac{1}{2} J_{cc}(0)].$$

If now we define

$$\delta\nu_{\parallel} \equiv \frac{3}{2} \delta\nu_c - \delta\nu_a, \quad (17)$$

we have

$$\delta\nu_{\parallel} = (2\hbar^2\sqrt{3})^{-1} J_{cc}(0). \quad (18)$$

Thus $\delta\nu_{\parallel}$ is the contribution to $\delta\nu_c$ from the longitudinal ($\parallel c$) local field fluctuations. In other words $\delta\nu_{\parallel}$ is the linewidth that would be observed with $\vec{H}_0 \parallel c$ if the effect of the transverse fluctuations could be suppressed.

V. DISCUSSION OF RESULTS

A. Temperature Dependence of $\delta\nu_{\parallel}$

Using the data of Fig. 1, we have calculated $\delta\nu_{\parallel}(T)$ from Eq. (17) over the temperature range $0.04 < T - T_N < 220$ °K. For the range $0.04 < T - T_N < 10$ °K the results are shown in Fig. 3. Since the data points for $\delta\nu_c$ and $\delta\nu_a$ were not taken at exactly the same set of temperatures, we computed $\delta\nu_{\parallel}$ by combining the data for $\delta\nu_c$ with the smoothed data for $\delta\nu_a$, giving the points denoted by the squares. Alternatively we combined the data for $\delta\nu_a$ with the smoothed (but not extrapolated) data for $\delta\nu_c$, giving the circles.

The critical behavior of $\delta\nu_{\parallel}$ is evidently well described by a power law. We made least-squares fits to the relation

$$\delta\nu_{\parallel}(T) = A[(T - T_N)/T_N]^{-n}. \quad (19)$$

For the range $0.04 < T - T_N < 10$ °K we found

$$n = 0.675 \pm 0.01, \quad A = (36.1 \pm 1.5) \text{ kHz}, \quad (20a)$$

while for the range $0.04 < T - T_N < 1.3$ °K we found

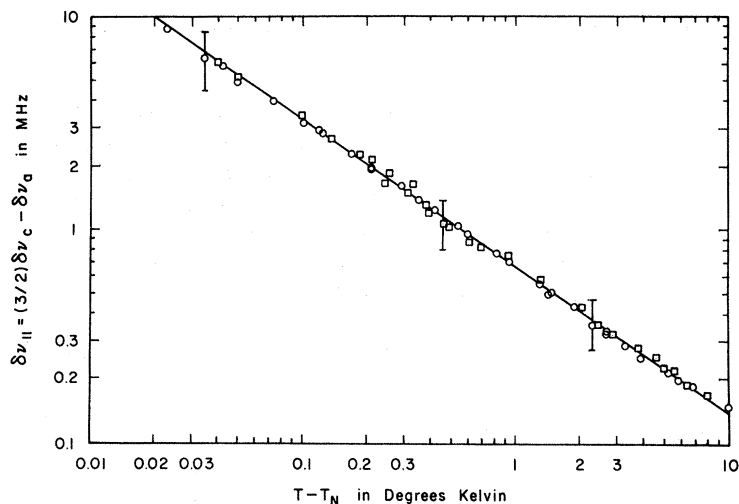


FIG. 3. Temperature dependence of the quantity $\delta\nu_{||}$ defined in Eq. (17) for $0.04 < T - T_N < 10$ °K. These values were computed from the data of Fig. 1 as discussed in the text. The quantity $\delta\nu_{||}$ corresponds through Eq. (18) to the low-frequency spectral density of the longitudinal component of the local field.

$$n = 0.670 \pm 0.02, \quad A = (37.1 \pm 4) \text{ kHz.} \quad (20b)$$

The error limits here correspond to two standard deviations. In these fits T_N was fixed³⁷ at the value determined by the independent method discussed in Sec. II.

The behavior of $\delta\nu_{||}(T)$ over a more extended range of temperature is plotted in Fig. 4, showing the breakdown of the power law further from T_N .

B. Dynamical-Scaling Theory for $\delta\nu_{||}(T)$

1. Outline of Relation to Scattering Function

Through Eq. (18), $\delta\nu_{||}$ corresponds to the fluctuations in the longitudinal component of the local field. If the nuclear-electronic couplings were isotropic, $\delta\nu_{||}$ would then be a measure of the longitudinal spin fluctuations. Thus, if each F^{19} nucleus

were isotropically coupled to the three near-neighbor²⁴ Fe^{2+} spins we would have^{3,19}

$$\delta\nu_{||}(T) \propto \int d^3K |A(\vec{K})|^2 S_{||}(\vec{K}, 0), \quad (21)$$

with

$$A(\vec{K}) = \sum_{n=1}^3 A_n e^{i\vec{K} \cdot \vec{r}_n},$$

where A_n is the coupling constant between a F^{19} nucleus and one of the neighboring electron spins situated relative to the nucleus at position \vec{r}_n . Here $S_{||}(\vec{K}, \omega)$ is the diffuse part of the Van Hove scattering function for the longitudinal spin fluctuation. It is clear physically that if the individual coupling tensors \vec{A}_n are not isotropic, the expression (21) should be modified to include a term containing the transverse scattering function, i.e., a contribution

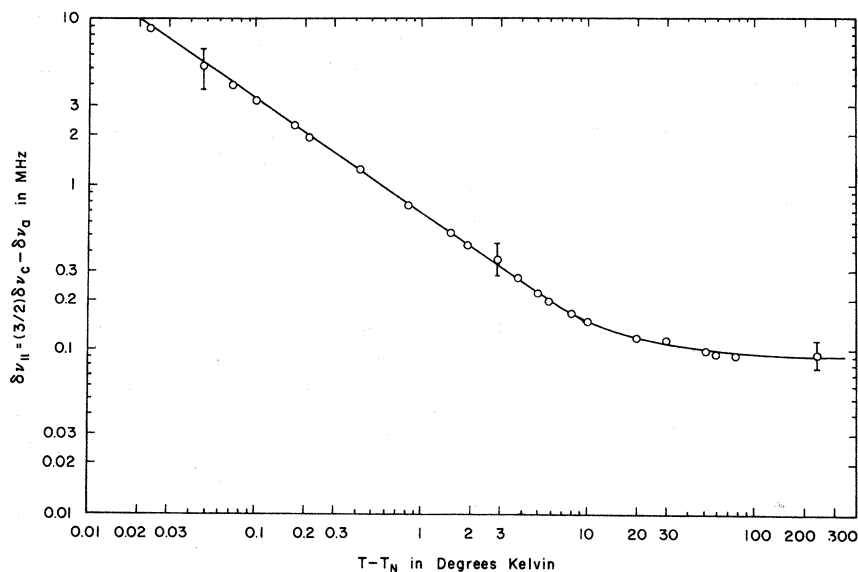


FIG. 4. Extension of our results for $\delta\nu_{||}(T)$ to the range $78.406 < T < 300$ °K, showing the breakdown of the critical-region power law at higher temperatures.

$$\int d^3K |B(\vec{K})|^2 S_L(\vec{K}, 0), \quad (22)$$

where $B(\vec{K})$ is essentially a Fourier transform of the nondiagonal part of the hyperfine coupling. While one may estimate that $|B(\vec{K})|^2$ may be as much as 10 or 20% of $|A(\vec{K})|^2$ for suitable \vec{K} , the arrangement of Fe^{2+} spins about each F^{19} site²⁴ is such that $B(\vec{K})$ vanishes exactly at $\vec{K} = \vec{K}_0$ = the antiferromagnetic mode. Since in the critical region most of the linewidth integral is due to modes near \vec{K}_0 (which we designate as $\vec{q} = 0$), the additional term (22) will be very small. In fact, for T near T_N we may adequately obtain the temperature dependence of $\delta\nu_{||}$ by replacing $A(\vec{K})$ by $A(\vec{K}_0)$ in (21). If in addition we relate^{3,19,20} $S_{||}(\vec{q}, 0)$ to the reduced longitudinal static susceptibility $\hat{\chi}_{||}(q, T) = \chi(q, T)/\chi_{\text{curie}}(T)$ and to the relaxation rate $\Gamma_{||}(q, T)$, we have simply

$$\delta\nu_{||}(T) \propto \int d^3q \frac{\hat{\chi}_{||}(q, T)}{\Gamma_{||}(q, T)}. \quad (23)$$

2. Interpretation of Power Law for $\delta\nu_{||}$

In the dynamical-scaling theory for an anisotropic system,¹⁴ there will be a region of the $(\kappa_{||}, q)$ plane near the origin for which the effects of anisotropy are dominant. There we can write

$$\Gamma_{||}(q, \kappa_{||}) = \kappa_{||}^z \Omega(q/\kappa_{||}). \quad (24)$$

For the uniaxial anisotropic antiferromagnet $\Omega(x)$ is a function tending to a nonzero value for $x \rightarrow 0$ and behaving asymptotically as x^z for large x , and

$$z = 2. \quad (25)$$

Using (24) and adopting the Ornstein-Zernike approximation for the static behavior,

$$\chi_{||}(q)/\chi_{||}(0) = [1 + (q/\kappa_{||})^2]^{-1},$$

the contribution to the linewidth integral (23) from all q values inside the sphere $|q| < q_0$ may be written

$$\delta\nu_{||}^{(q_0)}(T) \propto \hat{\chi}_{||}(0) \kappa_{||}^{3-z} \int_0^{q_0/\kappa_{||}} (1+x^2)^{-1} [\Omega(x)]^{-1} x^2 dx. \quad (26)$$

Writing the behavior of the reduced staggered susceptibility and inverse correlation range as $\hat{\chi}_{||}(0) \propto \epsilon^{-\tilde{\gamma}}$ and $\kappa_{||} \propto \epsilon^{-\nu}$, we then obtain the power law (19) with

$$n = \tilde{\gamma} - \nu(3-z). \quad (27)$$

This power law will be obtained only if the relation (24) and the approximation

$$A(\vec{K}_0 + \vec{q}) \cong A(\vec{K}_0) \quad (28)$$

are valid for all modes \vec{q} that contribute appreciably to the linewidth. [In this case the dependence of the integral in (26) on its upper limit will be slight.] If dynamical scaling is correct, these con-

ditions should hold for a suitably small temperature range above T_N . Actually we are a bit surprised that the power law exhibited in Fig. 3 holds over as wide a range as it does. We are currently making a more detailed comparison with the neutron scattering data¹⁶ in order to understand this, and to investigate the effect of the approximation (28).

Adopting (27) and taking $\tilde{\gamma} = \frac{4}{3}$ and $\nu = \frac{2}{3}$ for the exponents expressing the static properties, our experimental result (20b) leads to $z = 2.00 \pm 0.03$.

Alternatively, if we base our values of the static exponents on the scattering data,¹⁶ our result implies that

$$z = 2.0 \pm 0.25. \quad (29)$$

This supports the theoretical result (25) and overlaps with the results obtained in the scattering experiments,¹⁶ i. e., $z = 2.1 \pm 0.2$ from the q dependence of $\Gamma_{||}$ at T_N and $z = 2.3 \pm 0.4$ from the κ dependence of $\Gamma_{||}(q=0)$ above T_N .

In this connection we note that our experiment probes regions of the $(\kappa_{||}, q)$ plane which, on account of resolution limitations, were inaccessible in the neutron scattering work. We were able to take linewidth data to within 40 mdeg of T_N , at which point $\kappa_{||}$ was 0.0036 \AA^{-1} . The inaccessible region in the scattering work was a roughly elliptical portion of the $(\kappa_{||}, q)$ plane centered on $(0, 0)$ and of semiaxes $\approx 0.04 \text{ \AA}^{-1}$ along $\kappa_{||}$ and $\approx 0.06 \text{ \AA}^{-1}$ along q . Our power law (20b) was obtained entirely from data for which $0.0036 < \kappa_{||} < 0.04 \text{ \AA}^{-1}$. Also, our near-critical linewidths are dominated by modes $q < 0.02 \text{ \AA}^{-1}$, well inside the inaccessible region in the scattering experiment.

C. Discussion of Inequalities in Sec. IV

In this section we examine the inequalities which underlie the interpretation of our data for $\delta\nu_{||}(T)$ through Eq. (18). Consider first a comparison of the Larmor frequency with the local field fluctuation rate. There is no doubt that (14) is very well satisfied far above T_N , though it may break down close to T_N . We may obtain an approximate upper limit on the value of $\kappa_{||}$ for which this can occur as follows: At each temperature we write the longitudinal relaxation rate as

$$\Gamma_{||}(q, T) = \Gamma_{||}(0, T) + D(T) q^2$$

for small q . Then clearly the only modes q which can contribute to a discrepancy between $J_{cc}(0)$ and $J_{cc}(\omega_0)$ are those for which $D(T) q^2 \gtrsim \omega_0$ [although even these will not thus contribute if $\Gamma_{||}(0, T) \gg \omega_0$]. Since the effect of each mode in the linewidth integral is weighted by $\chi_{||}(\vec{q})$, it is clear that a breakdown of (14) requires

$$D(T) \kappa_{||}^2(T) \gtrsim \omega_0. \quad (30)$$

The scattering data,¹⁶ together with the assumption $z = 2.0$, suggest that D is of the order of a few meV \AA^2 over the temperature range of interest. Assuming this, for our high-field data ($\omega_0 \approx 3.7 \times 10^8 \text{ sec}^{-1}$), we then find $\kappa_{\parallel} \approx 0.01 \text{ \AA}^{-1}$ (or $T - T_N \approx 0.2 \text{ }^\circ\text{K}$), while for our low-field data ($\omega_0 \approx 9.4 \times 10^7 \text{ sec}^{-1}$) we find $\kappa_{\parallel} \approx 0.005 \text{ \AA}^{-1}$ (or $T - T_N \approx 0.07 \text{ }^\circ\text{K}$) for our upper limit estimates. Thus it is possible that the apparent failure of Eq. (4) for the data of Fig. 2 in the range $T - T_N < 0.2 \text{ }^\circ\text{K}$ may be explicable through $J_{cc}(\omega_0) < J_{cc}(0)$. On the other hand, the data do not force us to this conclusion: Indeed it is possible that the 15-kG field used in obtaining these data affected the Fe^{2+} spin correlation functions. If this effect changed upon rotating the field from c to a , a failure of (4) could result.

For the low-field data of Fig. 1, Eq. (14) may begin to break down for the data points closest to critical [although we see no significant breakdown of (4) at this level of accuracy]. Even if this happens, the interpretation of our results for $\delta\nu_{\parallel}$ through (18) is not invalidated. Indeed in this temperature region $J_{aa} \ll J_{cc}$. Then $\delta\nu_c$ (which is experimentally equal to $\delta\nu_{\parallel}$) is clearly a measure of $J_{cc}(0)$.

Now consider the requirement (13). For the data of Fig. 1, the minimum value of the left-hand side of (13) was 3.0. This occurred only for the $\vec{H}_0 \parallel c$ data closest to the critical point. [More generally (13) was well satisfied.] We now consider the ensuing systematic error. Just above T_N , where $J_{cc} \gg J_{aa}$, and with $\vec{H}_0 \parallel c$, the nuclear relaxation corresponds classically to a fanning-out of the Larmor precession angles in the transverse plane. In this case it may be shown²¹ that the relaxation function $R_{xx}(t)$ for a transverse component of the nuclear magnetization is still given rigorously by the Kubo-Tomita formula. We then write $R_{xx}(t) = \chi_0 e^{-t/T_2} \times \cos \omega_0 t$, where χ_0 is the static nuclear susceptibility. Employing the general Fourier transform relation³⁸ between the relaxation function and the nuclear absorption χ'' , we find

$$\chi''(\omega, \omega_0) = \frac{1}{2} \omega \chi_0 \left(\frac{1}{(\omega - \omega_0)^2 T_2^2 + 1} + \frac{1}{(\omega + \omega_0)^2 T_2^2 + 1} \right). \quad (31)$$

Thus in our field-sweep technique we should obtain a curve of nuclear absorption consisting of the sum of two Lorentzians respectively centered at equal positive and negative values of H_0 . The distinction between this situation and a single Lorentzian becomes academic for narrow lines. On refitting our

data on the basis of (31), rather than using a single Lorentzian as done originally, we find practically no change in our results.

Now we examine the condition (12) for a Lorentzian shape. This might possibly break down for the longitudinal local field fluctuation very close to T_N . We may expect that $J_{cc}(\omega)$ is a nonincreasing function of ω for small ω . Noting again that for our data $\omega_0 T_2$ always exceeded the value 3.0, we have $J_{cc}(1/T_2) \geq J_{cc}(3/T_2) \geq J_{cc}(\omega_0 T_2/T_2) = J_{cc}(\omega_0)$. Thus the low-Larmor-frequency condition (14) will break down before the Lorentzian condition (12) fails as $T \rightarrow T_N$. From our previous discussion of (14) we conclude that (12) is more than adequately satisfied at the accuracy level of the data of Fig. 1. Thus we can confidently interpret the data for $\delta\nu_{\parallel}(T)$ (Figs. 3 and 4) through Eq. (18).

VI. CONCLUSIONS

We have made a detailed experimental study of the F^{19} nuclear-resonance linewidth in the paramagnetic state of the anisotropic antiferromagnet FeF_2 . A pronounced anomaly is observed near the critical temperature. We conclude that the mechanism responsible for the observed linewidths is that of nuclear-electronic hyperfine coupling modulated by electron-spin motion. On this basis we provide a method for obtaining the portion of the linewidth $\delta\nu_{\parallel}$ due to the fluctuation in the longitudinal component of the local field. We conclude that $\delta\nu_{\parallel}$ corresponds to the low-frequency spectral density of the longitudinal component of the local field throughout the temperature range investigated. The critical behavior of $\delta\nu_{\parallel}$ is found to be quite well described by a power law. The data leading to this come from a range of temperatures quite close to T_N , and thus probe a region of the (κ_{\parallel}, q) plane which is largely inaccessible in a neutron scattering experiment. Subject to the approximations discussed in Sec. VB 2, the experimentally observed critical exponent for $\delta\nu_{\parallel}$ is in very good accord with predictions based on the theory of Riedel and Wegner.

ACKNOWLEDGMENTS

It is a pleasure to thank Dr. Franco Dupr e for his many valuable contributions to the initial phases of this work, Dr. Allan Mills for assistance in the design of some electronic apparatus, and Dr. M. P. Schulhof and Dr. E. K. Riedel for many helpful discussions.

*Work supported by the U. S. Air Force Office of Scientific Research, Grant No. AF68-1480.

†National Science Foundation Traineeship holder, 1965-1969.

¹L. P. Kadanoff, W. Gotze, D. Hamblen, R. Hecht, E. A. S. Lewis, V. V. Palciauskas, M. Rayl, J. Swift,

D. Aspnes, and J. Kane, *Rev. Mod. Phys.* **39**, 395 (1968).

²M. E. Fisher, *Rept. Progr. Phys.* **30**, 615 (1967).

³P. Heller, *Rept. Progr. Phys.* **30**, 731 (1967).

⁴S. M. Kulpa, *J. Appl. Phys.* **40**, 2274 (1969).

⁵W. Marshall and R. D. Lowde, *Rept. Progr. Phys.* **31**, 705 (1968).

- ⁶L. Van Hove, *Phys. Rev.* **95**, 1374 (1954).
- ⁷See, for example, N. C. Ford and G. B. Benedek, *Phys. Rev. Letters* **15**, 649 (1965); H. L. Swinney and H. Z. Cummins, *Phys. Rev.* **171**, 152 (1968).
- ⁸See Ref. 6 and also H. Mori and K. Kawasaki, *Progr. Theoret. Phys. (Kyoto)* **27**, 529 (1962); K. Kawasaki, *J. Phys. Chem. Solids* **28**, 1277 (1967).
- ⁹R. Nathans, F. Menzinger, and S. J. Pickart, *J. Appl. Phys.* **39**, 1237 (1968).
- ¹⁰H. Y. Lau, L. M. Corliss, A. Delapalme, J. M. Hastings, R. Nathans, and A. Tucciarone, *Phys. Rev. Letters* **23**, 1225 (1969).
- ¹¹R. A. Ferrell, N. Menyhard, H. Schmidt, F. Schwabl, and P. Szépfalusy, *Phys. Rev. Letters* **18**, 891 (1967).
- ¹²E. I. Halperin and P. C. Hohenberg, *Phys. Rev. Letters* **19**, 700 (1967); *Phys. Rev.* **177**, 952 (1969).
- ¹³R. Résibois and C. Piette, *Phys. Rev. Letters* **24**, 514 (1970).
- ¹⁴E. Riedel and F. Wegner, *Phys. Rev. Letters* **24**, 730 (1970); *Phys. Letters* **32A**, 273 (1970).
- ¹⁵A. Gottlieb, F. Dupré, and P. Heller, *J. Appl. Phys.* **40**, 1277 (1969).
- ¹⁶M. P. Schulhof, M. T. Hutchings, and H. J. Guggenheim, *J. Appl. Phys.* **42**, 1376 (1971) and private communications.
- ¹⁷M. P. Schulhof, P. Heller, R. Nathans, and A. Linz, *Phys. Rev. Letters* **24**, 1184 (1970); *Phys. Rev. B* **1**, 2304 (1970).
- ¹⁸P. Heller and G. B. Benedek, *Phys. Rev. Letters* **3**, 428 (1962).
- ¹⁹P. Heller, in *Critical Phenomena*, Natl. Bur. Std. (U. S.) Misc. Publ. No. 273, edited by M. S. Green and J. V. Sengers (U. S. GPO, Washington, D. C., 1966).
- ²⁰T. Moriya, *Progr. Theoret. Phys. (Kyoto)* **28**, 371 (1962).
- ²¹A. M. Gottlieb, thesis (Brandeis University, 1970) (unpublished).
- ²²See Ref. 21 for a detailed discussion of experimental techniques.
- ²³Y. Shapira, *Phys. Rev. B* **2**, 2725 (1970).
- ²⁴J. W. Stout and R. G. Shulman, *Phys. Rev.* **118**, 1136 (1960); V. Jaccarino, R. G. Shulman, and J. W. Stout, *Phys. Rev.* **106**, 602 (1957).
- ²⁵G. W. Smith, *J. Appl. Phys.* **35**, 1217 (1964).
- ²⁶G. V. H. Wilson, *J. Appl. Phys.* **34**, 3276 (1963).
- ²⁷H. Wahlquist, *J. Chem. Phys.* **35**, 1708 (1961).
- ²⁸R. Kubo and K. Tomita, *J. Phys. Soc. Japan* **9**, 888 (1954).
- ²⁹T. Moriya, *Progr. Theoret. Phys. (Kyoto)* **16**, 23 (1956); **16**, 641 (1956).
- ³⁰H. Suhl, *Phys. Rev.* **109**, 606 (1958); *J. Phys. Radium* **20**, 333 (1959); T. Nakamura, *Progr. Theoret. Phys. (Kyoto)* **20**, 542 (1958).
- ³¹According to Ref. 20, for $\vec{H}_0 \perp c$, the left-hand side of (5a) is reduced by about a factor of 2, while the left-hand side of (5b) is reduced by a factor much larger than 2. The coefficient on the right-hand side in (5a) is proportional to the square of the $F^{19}\text{-Mn}^{2+}$ hyperfine interaction. The coefficient on the right-hand side in (5b) is proportional to the product of the $F^{19}\text{-Mn}^{2+}$ and $\text{Mn}^{2+}\text{-Mn}^{55}$ hyperfine interactions. The values quoted in (5) neglect the narrowing effect of the $\text{Mn}^{55}\text{-Mn}^{55}$ coupling, which is absent for the $\text{Fe}^{57}\text{-Fe}^{57}$ case in FeF_2 . The results (5), which are valid asymptotically as $T \rightarrow T_N$ from above, probably underestimate the true effect for T well above T_N .
- ³²See M. E. Fisher and R. J. Burford, *Phys. Rev.* **156**, 583 (1967). See also, P. Heller, *Intern. J. Magnet.* (to be published).
- ³³T. Nagamiya, K. Yosida, and R. Kubo, *Advan. Phys.* **4**, 2 (1955).
- ³⁴P. Heller, *Phys. Rev.* **146**, 403 (1966).
- ³⁵In going from (8) to (11) we dropped a term of the form $-(2\hbar)^{-2} \int_{-\infty}^{\infty} \sin \omega_0 t \text{Im} \langle \{ \delta V_+(t) \delta V_-(0) \} \rangle dt$. In the paramagnetic state, and in zero applied field, this should indeed vanish as $\text{Im} \langle \{ \delta V_+(t) \delta V_-(0) \} \rangle$ is a measure of the tendency of the local field to precess in a definite sense about the z axis. With field applied to the electron-spin system this term will not vanish, though at low values of ω_0 it should be small compared to the terms retained in (11).
- ³⁶The form (11b) is clearly independent of the choice of axes in the xy plane; it also leads easily to an explicit expression for the dependence of $\delta\nu$ on the angular orientation of \vec{H}_{nuc1} , as we now show: Note first that $J_{\alpha\beta}(\omega) = J_{\beta\alpha}(\omega) = J_{\alpha\beta}^*(\omega)$ and that $J_{\alpha\beta}(\omega)$ transforms like a second-rank tensor. Choosing a coordinate system x_1, x_2, x_3 in which this tensor is diagonal, we find
- $$\delta\nu = (\pi/2\hbar^2) \left\{ \frac{1}{2} J(\omega_0) + [J_{33}(0) - \frac{1}{2} J_{33}(\omega_0)] (\hat{z} \cdot \hat{x}_3)^2 + [J_{22}(0) - \frac{1}{2} J_{22}(\omega_0)] (\hat{z} \cdot \hat{x}_2)^2 + [J_{11}(0) - \frac{1}{2} J_{11}(\omega_0)] (\hat{z} \cdot \hat{x}_1)^2 \right\}.$$
- This result may be visualized geometrically as follows: Construct a three-dimensional polar plot by assigning to every direction for \vec{H}_{nuc1} a length $r = (\delta\nu)^{-1/2}$. The resulting locus will be an ellipsoidal surface with principal axes x_1, x_2, x_3 . At low values of ω_0 , the ratio of any two principal dimensions of this ellipsoid cannot exceed $\sqrt{2}$.
- ³⁷Actually we made power-law fits to the $\delta\nu_c$ and $\delta\nu_d$ data in which T_N was treated as a free parameter. The values of T_N thus obtained agreed with (2) to within the experimental error of a few millidegrees.
- ³⁸See, for example, A. Abragam, *The Principles of Nuclear Magnetism* (Oxford U. P., Oxford, England, 1960), Chap. 4, Sec. B.